Structural changes in supercritical fluids at high pressures

Mario Santoro and Federico A. Gorelli
European Laboratory for Non Linear Spectroscopy (LENS), Via N. Carrara 1, I-50019 Sesto Fiorentino, Firenze, Italy and CNR —INFM CRS-SOFT, c/o Università di Roma "La Sapienza," I-00185 Roma, Italy
(Received 21 May 2008; published 25 June 2008)

The structure of an archetypal model simple fluid system as argon has been investigated by x-ray diffraction at high pressures and room and high temperatures. Despite the markedly supercritical conditions ($T=2-4T_c$, $P>10^2P_c$), the structure factor $S(Q)$ is very similar, close to the melting line, to that observed in the liquid phase, thereby assessing a liquidlike structure with high atomic correlation, as proposed in a recent inelastic experiment. On the other hand, the $S(Q)$ continuously changes upon approaching the extrapolation of the liquid-gas coexistence line in the $(P/P_c,\ T/T_c)$ plane, ultimately exhibiting low atomic correlation, which reasonably indicates intermediate character between liquid and gas. The analysis of the $S(Q)$s based on the hard-sphere model shows that the changes are driven by the decrease in the packing fraction and the increase in the nearest-neighbor distance with decreasing pressure.

DOI: 10.1103/PhysRevB.77.212103 PACS number(s): 62.50.−p, 61.05.cf, 61.20.−p, 81.30.Dz

The notion of critical temperature and pressure for the liquid-gas phase transition dates back to the 19th century and is broadly discussed in thermodynamics textbooks (see, for instance, Zemanski[1]). It is well assessed that the critical temperature parts the phase diagram of fluids into a subcritical two phases region and a supercritical single phase region. The supercritical fluid exhibits intermediate physical properties between those of liquid and gas. Nevertheless, the questions arise on what extent do subcritical properties persist in the single phase region far beyond the critical point; and whether or not it is still possible to identify a liquidlike and a gaslike subregion having structural and dynamical properties resembling those of liquids and gases, respectively; and how, if so, those regions would connect each other in the phase diagram. Indeed, a variety of studies have been performed through the years on fluids around the critical point and also above the critical temperature (see references in Ref. 2). Unfortunately, the experimental investigations performed so far provided very limited knowledge of the deep supercritical region, since hydrothermal cells, which only work in the range of 10–1000 bar, have been usually employed. On the other hand, the rapid development of high-pressure techniques based on diamond-anvil cells (DACs) joined to the cutting edge modern synchrotron techniques have made possible the investigation of structural and dynamical properties of markedly supercritical fluids. In a recent study on highly supercritical oxygen ($T\approx 2T_c$, $P>10^3P_c$), based on measurements of the dynamic structure factor $S(Q,\omega)$ performed through the inelastic x-ray scattering (IXS), we found that sound velocity in the terahertz regime exceeds the hydrodynamic value of about 20%, a feature which is the fingerprint of liquidlike dynamics.[2] The comparison of results on oxygen with literature data obtained in several fluids led us to suggest that the end of the liquid dynamics is not marked only by the critical temperature and to indicate that the extrapolation of the liquid-gas coexistence line in the supercritical region of the P-T phase diagram (corresponding to the Widom's line, i.e., to the locus of the specific-heat maxima) as the relevant edge between liquidlike and gaslike dynamics. A connection of the Widom's line with the dynamic crossover was also theoretically predicted in systems with a liquid-liquid phase transition.[3] It was then a relevant open question whether the liquidlike and gaslike regions could be actually identified on the basis of structural modifications, which can be shown by measurements of the static structure factor $S(Q)$ through x-ray diffraction (XRD), thereby complementing the dynamical study. Also, a broad and dense mapping of the phase diagram is rather difficult in IXS measurements, since the signal is very low and 12–15 h are needed for each P-T point. Furthermore, the accuracy of the IXS is rather poor in DACs, close to the Widom's line (0.05–0.5 GPa), e.g., to the possible gaslike regime, due to the relatively low densities; here, the signals become exceedingly weak and the inelastic-scattering peaks merge to the elastic line, making the determination of the velocity of sound difficult. These reasons motivated an extended investigation of the deep supercritical region of fluids by XRD. Indeed, XRD studies of supercritical fluids in DACs have been very limited so far. In two recent works, the $S(Q)$ was determined in argon and oxygen at one thermodynamic point and at several P-T points, respectively, close to the melting line in the 1–6 GPa pressure range.[4,5] In these studies, the $S(Q)$ is very similar to that of the liquid. This kind of study is a challenging task to accomplish due to the limited sample size, the huge background signal from diamonds, and the limited accessible Q range, while small sample sizes make neutron diffraction simply impossible.

In this Brief Report, we investigate the static structure factor of a model gaseous system as argon, in the deep supercritical region in the P-T range of 0.4–4 GPa and 298–600 K. The study extends from the melting to the Widom's line. Continuous changes are observed between a highly atomic correlated liquidlike structure and a weakly atomic correlated structure close to the two lines. The more disordered structure reasonably indicates the intermediate character between liquid and gas. In Fig. 1 our P-T points in the reduced P/P_c-T/T_c phase diagram are reported. The experimental $S(Q)$ was fitted to a theoretical $S(Q)$ obtained through the hard-sphere model, which provided clues on the microscopic mechanism underlying the structural changes.

We have used a membrane type DAC equipped with 600 μm culet diamonds glued on tungsten carbide seats and Inconel 718 gaskets. A uniform resistive heating was provided by a hot ring clamped around the DAC. The cell was

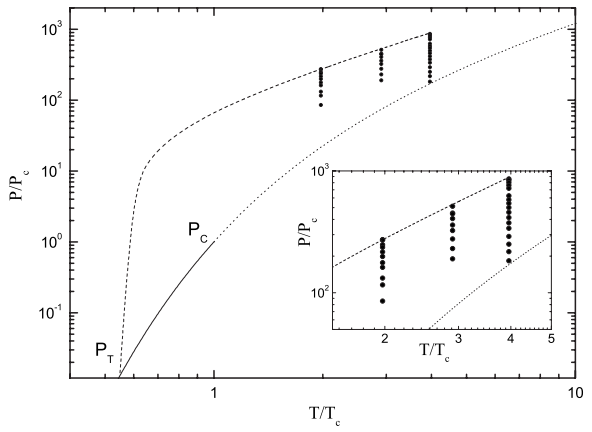

FIG. 1. P-T points (dots) where the $S(Q)$ has been measured, in the reduced $(P/P_c\text{-}T/T_c)$ plane. Inset: Enlarged region of the plane. Continuous and dotted line: Best fit to the average of the liquid-vapor coexistence line for several simple gaseous systems, including argon, neon, nitrogen, and oxygen, drawn below (continuous line) and extrapolated above (dotted line, approximation of the Widom's line) the critical point P_C (Ref. 2). Dashed line: Melting curve of argon extending from the triple point P_T (Refs. 7 and 20).

gas loaded with Ar at 1200 bar. The sample was about 300 μm in diameter and 50 μm thick. A chip of $SrB_4O_7:Sm^{2+}$ was inserted in the sample chamber for measuring pressures based on the shift of the $^5D_0$-$^7F_0$ fluorescence line.[6] Temperatures were determined by a K-type thermocouple placed very close to one diamond and were checked with the known melting curves of argon.[7] The XRD was performed along three isothermal pressure scans: at room temperature T (298 K), 438 K, and 597 K. Solid argon was melted along isothermal decompression under visual inspection. The fluid state was then obtained very close to the melting line at 1.3–4.2 GPa, depending on temperature, and XRD was done upon decreasing pressure down to a few tenths of gigapascals. Angle dispersive XRD has been measured at the ID09A beamline of the ESRF with a monochromatic beam (λ=0.3731 Å) and image-plate detection. The beam spot at the sample was 60 μm in diameter. We accessed a maximum diffraction angle 2θ of about 18°. The diffraction patterns were analyzed and integrated by means of the FIT2D computer code[8] to obtain the one-dimensional intensity distribution, corrected for the polarization dependent Thompson scattering factor as a function of the 2θ scattering angle and, consequently, of the momentum transfer $Q=(4\pi/\lambda)\sin\theta$.

The scattered intensity from the sample, I_s, has been obtained as $I_s=I-\alpha I_b$, where I is the total scattered intensity, I_b is the empty cell background intensity due to the Compton scattering from diamond anvils, and the scaling factor α takes into account variations in the synchrotron intensity. The αI_b term is about 1.6–8 times the I_s term at the first sharp diffraction peak (FSDP). The coherent sample intensity I_{coh} is then obtained as $I_{\text{coh}}=I_s-I_{\text{incoh}}$, where I_{incoh} is the incoherent Compton sample intensity. Finally, the static structure factor $S(Q)$ is obtained as

$$S(Q)=A\frac{I_{\text{coh}}}{f_{\text{coh}}^2}=A\frac{(I_s-\beta R f_{\text{incoh}}^2)}{f_{\text{coh}}^2}, \tag{1}$$

where A is a normalization factor, f_{coh} and f_{incoh} are the coherent and incoherent atomic form factors,[9] respectively, $R=(\lambda'/\lambda)^2$ is the Breit-Dirac inelastic correction factor with λ' and λ as the Compton scattered and the incident wavelengths, respectively, and β is a scaling factor that has to be adjusted in order to evaluate the correct values of I_{incoh}. The β and A factors have been determined in order to make the $S(Q)$ asymptotically oscillating around 1 at high Qs beyond the FSDP.

In Fig. 2 we report some high-pressure $S(Q)$s measured along the three isotherms along with the $S(Q)$ in the liquid phase[10] close to the liquid-gas-solid triple point. In the available Q range, we observe the FSDP at 20–23 nm^{-1} and the first high Qs oscillation. The peaks and the minima of high-pressure $S(Q)$s are shifted toward high Qs by 3–6 nm^{-1}, with respect to the triple point $S(Q)$, due to the higher den-

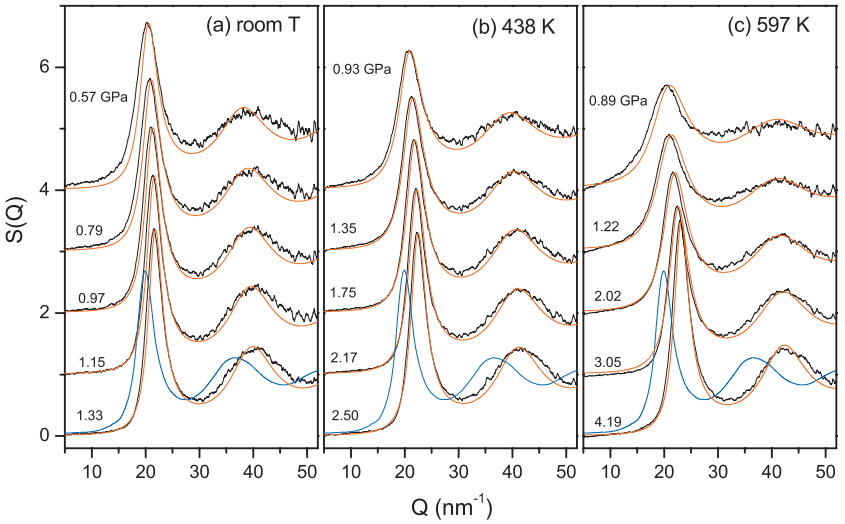

FIG. 2. (Color) Some high pressure $S(Q)$s measured along three isotherms (black lines). Blue lines: $S(Q)$ in the liquid (Ref. 10) close to the liquid-gas-solid triple point. Red lines: Fit of Eq. (2) to the experimental $S(Q)$s. The $S(Q)$s have been offset by 1 for clarity.

sity, and they move toward lower momentum-transfer values upon decreasing pressure. The $S(Q)$s measured close to the melting line are very similar to that of the liquid, which strongly suggests that the microscopic structure of the supercritical fluid is liquidlike, retaining the typical cooperative nature of the liquids. On the other hand, the contrast of the $S(Q)$ tends to vanish upon approaching the Widom's line, as shown by the decrease in the intensity of the FSDP and of the intensity difference between maxima and minima in the high Q oscillation. This behavior suggests that the cooperative nature of the structure tends to vanish. In order to make the discussion more quantitative, we operatively define a contrast parameter γ of the high Q oscillation of the $S(Q)$ as $\gamma=(S_{I\,\max}-S_{I\,\min})/S_{I\,\min}$, where $S_{I\,\max}$ and $S_{I\,\min}$ are the $S(Q)$ values at the first maximum, around 39–43 nm^{-1}, and at the first minimum, around 29–32 nm^{-1}, respectively. In Fig. 3 we report the γ parameter vs pressure for the three isotherms. We note that the contrast value close to the high-pressure melting points is higher than that observed in the liquid at the triple point. It is then shown that the contrast goes to zero upon decreasing pressure (at the Widom's line, it is decreased by almost 1 order of magnitude), following a linear fit with the intercept value fixed to zero. It also results that the slope δ of the γ vs P behavior does increase upon decreasing the temperature, e.g., the pressure driven structural changes become sharper and sharper upon approaching the critical point, as one may expect if the Widom's line would mark a sluggish liquidlike-gaslike transformation mimicking the subcritical liquid-gas phase transition. This aspect is emphasized in the inset of Fig. 3, where we report the $1/\delta$ parameter as a function of temperature. A linear law has been fitted through the points, whose extrapolation to the $1/\delta=0$ value ($\delta=\infty$) is indeed very close to the critical temperature.

A relevant insight to the structural changes is provided by analyzing the experimental $S(Q)$s based on the known solution of the Percus-Yevick equation[11,12] for the hard-sphere model. This kind of solution has been summoned by Ashcroft *et al.*,[13] who successfully fitted the model $S(Q\sigma)$, where σ is the hard-sphere diameter, to the experimental structure factor of many liquid metals. The hard-sphere $S(Q\sigma)$ is given by[13]

$$S(Q\sigma)=\left[1+24\eta\int_0^1 s^2\frac{\sin sQ\sigma}{sQ\sigma}(a+bs+cs^3)ds\right]^{-1}, \quad (2)$$

where $\eta=(\pi/6)n\sigma^3$ is the packing-density parameter, e.g., the fraction of total fluid volume occupied by the spheres; n is the numerical density; and a, b, and c are functions of η. The evaluation of $S(Q\sigma)$ from Eq. (2) is straightforward in terms of elementary functions. This model is dependent only on the value of η. Experimental $S(Q)$s for alkali metals at ambient pressure, close to the melting point are well reproduced by Eq. (2) with $\eta=0.45$ (Ref. 13), a value indicating close packing. The model has been recently extended to fit the experimental $S(Q)$s of liquid Cs (Ref. 14) and iron (Ref. 15) at high pressures and temperatures close to the melting line. The fit was rather successful by keeping η essentially constant with pressure, equal to 0.45 for Cs and to 0.43–0.44 for iron, and by decreasing the hard-sphere diameter σ with increasing pressure. Indeed, in this oversimplified model, the σ states the P-T dependent nearest-neighbor distance; this is the reason why it does depend on the thermodynamic point. We fitted Eq. (2) to our $S(Q)$s of argon at all the investigated P-T points, both close and far away from the melting line, by letting η change with pressure in order to reproduce the changing contrast. Indeed, η was the only fitting parameter, and σ was obtained from η, having inferred the density values from the literature. The high-pressure equation of state (EOS) of fluid argon is known only up to 1.0–1.3 GPa, from low temperatures up to 400 °C.[16–18] We extrapolated the EOS data toward higher pressures in the whole P-T range of this study by fitting the available P-V-T data to the same law that was adopted for fitting the EOS of fluid N_2 (Ref. 19), $V=AP^B+C\ln P+D/P+E/P^2+F$, where the parameters $A-F$ depend on temperature. In Fig. 2 the model $S(Q)$s that were successfully fitted to the experimental data are reported, and in Fig. 4 the pressure behavior of the η and σ parameters for the three isotherms is shown. The agreement between the model and the measured structure factors gets slightly worse upon decreasing pressure in terms of contrast and peak positions, which is most likely to be due to the soft-sphere details of the true interatomic potential becoming increasingly relevant. The η parameter is equal to about 0.50 close to the melting points. This value is higher than that at the triple point (0.46), and even higher than that of liquid metals, and it clearly points to a highly close-packed fluid. The η then decreases with pressure, falling down to about 0.34 close to the Widom's line, as found in the 597 K isotherm. The decreasing behavior of η with decreasing pressure is paralleled by the opposite behavior of σ, which roughly represents the true nearest-neighbor distance. This parameter

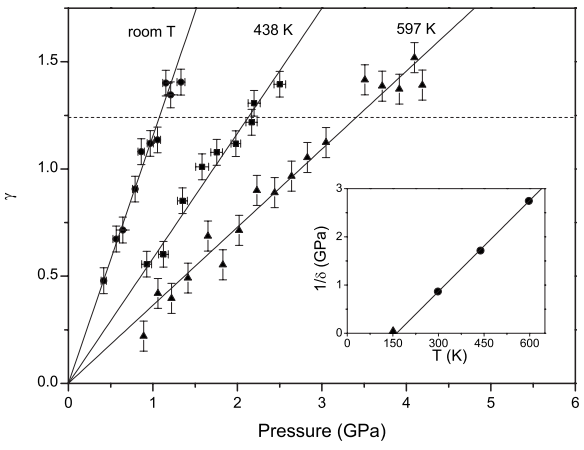

FIG. 3. Contrast γ parameter (see text) versus pressure at room T (circles), 438 K (squares), and 597 K (triangles). Continuous lines: Linear fit to the data with slope δ and with the intercept value fixed to zero. Dashed line: Value of γ for the liquid close to the triple point. Error bars on γ reflect the errors on α, A, and β [see text and Eq. (1)], and the noise in the $S(Q)$. Pressure error bars are due to the inaccuracy in measurements of the $SrB_4O_7:Sm^{2+}$ fluorescence and to the pressure changes during one single XRD measurement. Inset: Inverse of the δ parameter as a function of the temperature; a linear law has been fitted through the points. The critical temperature is also indicated (triangle). Error bars on $1/\delta$ and T are of the order of the point size.

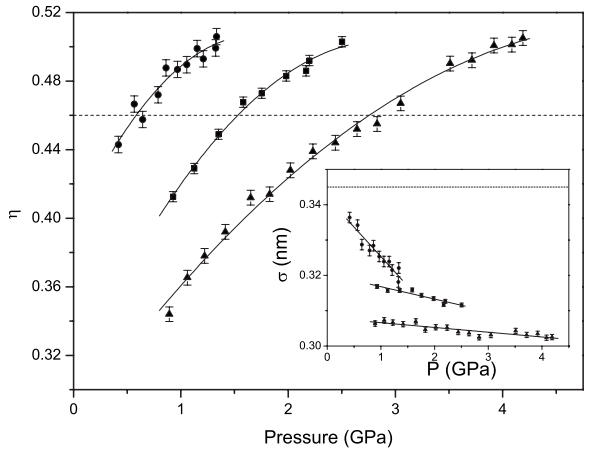

FIG. 4. Pressure behavior of the η and σ (inset) parameters of the hard-sphere model at room temperature T (circles), 438 K (squares), and 597 K (triangles). A second-order polynomial and a linear law were fitted through the points for η and σ, respectively (continuous lines). Dashed lines: Values of η and σ in the liquid close to the triple point.

ranges from about 0.302 to 0.336 nm, at the highest and the lowest P-T points, respectively. The last value is close to that obtained at the triple point, equal to 0.345 nm. We note that the slope of the pressure dependence of σ increases with decreasing temperature. We think that the reason for this could be properly understood only *a posteriori*, after having tried to reproduce the experimental $S(Q)$s by means of more realistic soft potentials, which in turn is beyond the scope of our work.

In conclusion, we have investigated the high-pressure behavior of the microscopic structure of a model fluid system, argon, in the deep supercritical P-T region. The study of the $S(Q)$ extends from the melting line to the Widom's line. It has been shown that the character of fluids continuously changes upon reducing pressure from a highly atomic correlated, cooperative, and liquidlike nature, close to the melting line, to a weakly atomic correlated nature, close to the Widom's line. It has also been shown, in the framework of the hard-sphere model, that the changes are driven by the decrease in pressure of the packing fraction of the fluid, paralleled by an increase in the hard-sphere diameter, e.g., of the nearest-neighbor distance. This study complements an investigation on the nature of supercritical fluids in a more limited P-T range, based on the microscopic dynamical properties.[2] It is still an open question, from the structural point of view, whether the Widom's line marks a sluggish liquidlike-gaslike transformation mimicking the subcritical liquid-gas phase transition, as proposed in the dynamical study. If this is the case, then the P-T range of the transformation crossing the Widom's line would include the low-pressure side of the P-T range of this work. Indeed, this point is reasonable, since the low atomic correlated structure observed close to the Widom's line is indicative of the intermediate character of the fluid between liquid and gas and, ultimately, of a possibly developing gaslike character beyond this line. In order to address this issue, it will be of crucial importance the structural investigation of the possible deep supercritical gaslike regime, beyond the Widom's line, where the density is low and much bigger sample volumes than those allowed by the DACs are needed for getting reliable scattered signals. We hope that our work will stimulate these additional investigations. In fact, much deeper knowledge than ever could be achieved on the supercritical region of phase diagrams.

We acknowledge the ESRF for provision of beam time at ID09A, and M. Hanfland and M. Merlini for their help in sample preparation and XRD measurements. This work was supported by the European Community under Contract No. RII3-CT2003-506350.

[1] M. W. Zemanski, *Heat and Thermodynamics* (MacGraw-Hill, New York, 1968).
[2] F. Gorelli, M. Santoro, T. Scopigno, M. Krisch, and G. Ruocco, Phys. Rev. Lett. **97**, 245702 (2006).
[3] L. Xu, P. Kumar, S. V. Buldyrev, S.-H. Chen, P. H. Poole, F. Sciortino, and H. E. Stanley, Proc. Natl. Acad. Sci. U.S.A. **102**, 16558 (2005).
[4] J. H. Eggert, G. Weck, P. Loubeyre, and M. Mezouar, Phys. Rev. B **65**, 174105 (2002).
[5] G. Weck, P. Loubeyre, J. H. Eggert, M. Mezouar, and M. Hanfland, Phys. Rev. B **76**, 054121 (2007).
[6] F. Datchi, R. Le Toullec, and P. Loubeyre, J. Appl. Phys. **81**, 3333 (1997).
[7] F. Datchi, P. Loubeyre, and R. Le Toullec, Phys. Rev. B **61**, 6535 (2000).
[8] A. P. Hammersley, S. O. Svensson, M. Hanfland, A. N. Fitch, and D. Häusermann, High Press. Res. **14**, 235 (1996).
[9] A. J. C. Wilson and E. Price, *International Tables for Crystallography* (Kluwer, Dordrecht/International Union of Crystallography, The Netherlands, 1999), Vol. C.
[10] J. L. Yarnell, M. J. Katz, R. G. Wenzel, and S. H. Koenig, Phys. Rev. A **7**, 2130 (1973).
[11] J. K. Percus and G. J. Yevick, Phys. Rev. **110**, 1 (1958).
[12] P. A. Egelstaff, *An Introduction to the Liquid State*, 2nd ed. (Oxford Science Publications, Oxford, 1992).
[13] N. W. Ashcroft and J. Lekner, Phys. Rev. **145**, 83 (1966).
[14] S. Falconi, L. F. Lundegaard, C. Hejny, and M. I. McMahon, Phys. Rev. Lett. **94**, 125507 (2005).
[15] G. Shen, V. B. Prakapenka, M. L. Rivers, and S. R. Sutton, Phys. Rev. Lett. **92**, 185701 (2004).
[16] S. L. Robertson, S. E. Babb, Jr., and G. J. Scott, J. Chem. Phys. **50**, 2160 (1969).
[17] M. Grimsditch, P. Loubeyre, and A. Polian, Phys. Rev. B **33**, 7192 (1986).
[18] C. A. ten Seldam and S. N. Biswas, J. Chem. Phys. **94**, 2130 (1991).
[19] R. L. Mills, D. H. Liebenberg, and J. C. Bronson, J. Chem. Phys. **63**, 1198 (1975).
[20] W. H. Hardy, R. Crawford, and W. Daniels, J. Chem. Phys. **54**, 1005 (1971).